Redox Biology 64 (2023) 102782

Contents lists available at ScienceDirect

Redox Biology

journal homepage: www.elsevier.com/locate/redox

CircRNA Galntl6 sponges miR-335 to ameliorate stress-induced hypertension through upregulating Lig3 in rostral ventrolateral medulla

Shuai Zhang [a], Xueping Wang [b], Gaojun Chen [b], Lei Tong [b], Tengteng Dai [b], Linping Wang [b], Liucun Zhu [b], Haili Zhang [c], Dongshu Du [b,c,d,*]

[a] International Cooperation Laboratory of Molecular Medicine, Academy of Chinese Medical Sciences, Zhejiang Chinese Medical University, Hangzhou, Zhejiang, 310053, China
[b] College of Life Sciences, Shanghai University, Shanghai, 200444, China
[c] College of Agriculture and Bioengineering, Heze University, Heze, Shandong, 274015, China
[d] Shaoxing Institute of Shanghai University, Shaoxing, Zhejiang, 312000, China

ARTICLE INFO

Keywords:
CircRNA Galntl6
Lig3
miR-335
Rostral ventrolateral medulla
Stress-induced hypertension

ABSTRACT

Rostral ventrolateral medulla (RVLM) is thought to serve as a major vasomotor center that participates in controlling the progression of stress-induced hypertension (SIH). Circular RNAs (circRNAs) perform important functions in the regulation of diverse physiological and pathological processes. However, information concerning the functions of RVLM circRNAs on SIH remains limited. RNA sequencing was performed to profile circRNA expression in RVLMs from SIH rats, which were induced by electric foot shocks and noises. The functions of circRNA Galntl6 in reducing blood pressure (BP) and its potential molecular mechanisms on SIH were investigated via various experiments, such as Western blot and intra-RVLM microinjection. A total of 12,242 circRNA transcripts were identified, among which circRNA Galntl6 was dramatically downregulated in SIH rats. The upregulation of circRNA Galntl6 in RVLM effectively decreased the BP, sympathetic outflow, and neuronal excitability in SIH rats. Mechanistically, circRNA Galntl6 directly sponged microRNA-335 (miR-335) and restrained it to reduce oxidative stress. Reintroduction of miR-335 observably reversed the circRNA Galntl6-induced attenuation of oxidative stress. Furthermore, Lig3 can be a direct target of miR-335. MiR-335 inhibition substantially increased the expression of Lig3 and suppressed oxidative stress, and these favorable effects were blocked by Lig3 knockdown. CircRNA Galntl6 is a novel factor that impedes SIH development, and the circRNA Galntl6/miR-335/Lig3 axis represents one of the possible mechanisms. These findings demonstrated circRNA Galntl6 as a possibly useful target for the prevention of SIH.

1. Introduction

Hypertension, defined as blood pressure (BP) $\geq$ 140/90 mmHg, has been associated with numerous health problems, such as kidney damage and stroke [1,2]. Estimates suggest that 1.39 billion people globally had hypertension in 2010, and by 2025, the number of adults with hypertension will reach 1.56 billion [3,4]. Hypertension is attributed to several causes, such as high salt intake [5]. Excessive stress is also related to a high BP [6,7], a condition known as stress-induced hypertension (SIH). Hyperactivation of the autonomic nervous system and its sympathetic arm has been demonstrated in hypertension [8]. Stressors activate the sympathetic nervous system, and this response is thought to be the primary cause of SIH [9].

Cardiovascular centers, which regulate sympathetic outflow and BP and include the nucleus tractus solitarius (NTS), rostral ventrolateral medulla (RVLM), and caudal ventrolateral medulla (CVLM), are present in the medulla oblongata [10]. RVLM is the major source of raised sympathetic outflow in hypertensive states [11]. Ooi et al. revealed that the activation of sigma-1 receptor in RVLM can restrain neuroinflammation and sympathetic hyperactivity, which ameliorates SIH [12]. Chronic stress activates the angiotensin II/Toll-like receptor 4/MyD88/nuclear factor-kappa B axis in RVLM, which can enhance sympathetic activity, leading to SIH progression [13]. NaV1.6 dysregulation in RVLM excites the sympathetic nerve and promotes SIH development [14]. Abnormal expressions of numerous genes induced by stress in the RVLM participate in the genesis of SIH. Thus, the molecular regulatory mechanisms underlying the gene expression in RVLM must

* Corresponding author. College of Life Sciences, Shanghai University, Shanghai, 200444, China.
E-mail addresses: dsdulab@163.com, dsdu@shu.edu.cn (D. Du).

https://doi.org/10.1016/j.redox.2023.102782
Received 2 May 2023; Received in revised form 8 June 2023; Accepted 8 June 2023
Available online 9 June 2023

Abbreviations

BP	blood pressure
CAT	catalase
ceRNA	competing endogenous RNA
CircRNA	circular RNA
CVLM	caudal ventrolateral medulla
DCF	dichlorofluorescein
DHE	dihydroethidium
ELISA	enzyme-linked immunosorbent assay
FISH	fluorescence in-situ hybridization
HR	heart rate
HRP	horseradish peroxidase
MAP	mean arterial pressure
MiR-335	microRNA-335
MMP	mitochondrial membrane potential
MUT	mutant
NC	negative control
ncRNA	Noncoding RNA
NE	norepinephrine
NTS	nucleus tractus solitarius
PBS	phosphate buffered saline
PVN	paraventricular nucleus
RAS	renin-angiotensin-aldosterone system
RSNA	renal sympathetic nerve activity
ROS	reactive oxygen species
RT-qPCR	reverse transcription quantitative polymerase chain reaction
RVLM	rostral ventrolateral medulla
SEM	standard error of the mean
SFO	subfornical organ
SIH	stress-induced hypertension
SNA	sympathetic nerve activity
SOD	superoxide dismutase
WT	wild-type
8-OH-dG	8-hydroxydeoxyguanosine

be clarified to improve SIH.

Noncoding RNAs (ncRNAs) are a large segment of the transcriptome that lacks protein coding capacity; however, they have been confirmed to regulate gene expression at the transcriptional, post-transcriptional, and translational levels [15]. Circular RNAs (circRNAs) are a subset of ncRNAs without a 5′ cap and a 3′ tail, and they are implicated as key regulatory molecules in diverse pathological and physiological processes [16]. Numerous peripheral circRNAs, such as circRNA 0016070, circRNA sirtuin 1, and circRNA 0014243, are crucial in hypertension development [17–19]. However, studies on the characterization of circRNA profiles in cardiovascular centers and their functions in sympathetic outflow and BP have not been reported. To date, no research has identified the expression patterns of circRNAs in RVLM and determined their regulatory roles.

In this study, thousands of distinct circRNAs were identified by analyzing the RVLM tissue isolated from SIH and control rats via RNA sequencing, and the results demonstrated the significantly downregulated expression of circRNA Galntl6 in SIH rats. The effects of circRNA Galntl6 overexpression on oxidative stress, neuronal excitability, sympathetic discharges, and BP were revealed. Whether circRNA Galntl6 is a sponge of miR-335-targeted Lig3 was determined. Moreover, the effects caused by miR-335 and circRNA Galntl6 or Lig3 on oxidative stress and SIH progression were illustrated. To the author's knowledge, this work is the first to reveal a comprehensive data framework for the exploration of RVLM circRNA changes accompanying abnormal BP in SIH pathogenesis. The findings shed a novel light on the pathophysiologic mechanism of SIH and provide a new therapeutic target for the treatment of SIH.

2. Materials and methods

2.1. Animals

A total of 150 male Sprague–Dawley rats (7 weeks old, pathogen and virus free), with an average weight of 230–260 g and obtained from Beijing Vital River Laboratory Animal Technology Co., Ltd., were used in this study. The animals were maintained at an ambient temperature of 23 °C ± 1 °C, a relative humidity of 50%–60%, and a 12-h light–dark period in the laboratory animal center of Shanghai University. One rat was housed per cage and given chow food and water ad libitum. The animals were arbitrarily allocated to different experimental groups. All animal studies were approved by the Animal Care Ethics Committee of Shanghai University (APPROVAL ID: SYXK (HU) 2019–0020) and performed in accordance with the international guidelines on the ethical use of animals [20,21]. A SIH rat model was established based on previous publications [14,22]. In brief, the rats in the stressed groups were placed in a cage (with length, width, and height of 22, 22, and 28 cm, respectively) with a grid floor and exposed to electric foot shock (35–80 V for a duration of 50–100 ms, with an interval of 2–30 s duration controlled by a computer) combined with buzzer noise stress administered for 2 h twice a day (9–11 a.m. and 3–5 p.m.) with a 4 h interval between sessions for 15 consecutive days. The rats in the control group were placed in cages for the same period, but they were neither subjected to electric foot shocks nor buzzer noises.

2.2. Cell culture

The rat neuroblastoma B104 cell line used in this research was purchased from Shanghai Xuanya Biotechnology Co., Ltd. and authenticated by the supplier. The cells were maintained in high-glucose Dulbecco's Modified Eagle's Medium (Thermo Scientific, USA) supplemented with 10% fetal bovine serum (Thermo Scientific, USA) at 37 °C in 5% CO_2.

2.3. Measurement of BP and heart rate (HR)

The radiotelemetry system (Kaha Sciences, New Zealand) was employed to measure the BP and HR of conscious rats. In brief, the telemeter catheter was inserted into the abdominal aorta of rats and fixed with a tissue adhesive and a mesh patch under inhalational anesthesia with isoflurane (oxygen flowmeter turned to 0.8–1.5 L/min; isoflurane vaporizer turned to 3%–5%). We then secured the body of the telemeter to the peritoneum. Afterward, the rats were given 1 week to recover from the surgery before recording began. The signals of BP and HR were received by SmartPad (Kaha Sciences, New Zealand), and data were collected in a fixed period of 3 h (8–11pm) every day using the PowerLab system (AD Instruments, Australia) for 6 days before (baseline) and 15 days after stress.

2.4. Recording of renal sympathetic nerve activity (RSNA)

The RSNA was recorded as previously described [14,22]. In brief, the left renal sympathetic nerve was carefully isolated through incision surgery under isoflurane anesthesia as above and placed on a pair of platinum-iridium electrodes. Next, the nerve-electrode complex was covered by Kwik-Sil gel (World Precision Instruments, USA). A grass P55C preamplifier was then used to amplify and filter the nerve activity. The signal was acquired and integrated using the PowerLab system (AD

Instruments, Australia) for 1 h. The maximum nerve activity was detected 1–2 min after the rats were overdosed with ≥150 mg/kg intra-peritoneal (i.p.) pentobarbital sodium. At 20–30 min after the rats were sacrificed, the background noise level of the nerve activity was calculated. Baseline RSNA was considered a percentage of maximum after subtracting the background noise.

2.5. Plasma norepinephrine (NE) determination

Blood was collected from isoflurane-anaesthetized rats by cardiac puncture into collection tubes (added with ethylenediaminetetraacetic acid) and immediately centrifuged at 1000×*g* for 15 min at 4 °C, and the supernatant was used for detection. An enzyme-linked immunosorbent assay (ELISA) kit (FineTest, China) was utilized to measure the level of plasma NE in accordance with the manufacturer's instructions.

2.6. Immunofluorescence

Rats were perfused transcardially with 200 mL heparinized saline and 200 mL freshly prepared 4% paraformaldehyde through the ascending aorta under pentobarbital sodium anesthesia (50 mg/kg, i.p.). The brains were carefully removed, post-fixed for 12 h in 4% paraformaldehyde at room temperature, and dehydrated with 20% sucrose overnight at 4 °C. Afterward, they were placed in 30% sucrose for further dehydration overnight at 4 °C. Next, 30 μm-thick frozen coronal sections containing RVLM were cut using a cryostat (Thermo Scientific, USA). The sections were permeabilized with 0.3% Triton X-100 for 10–15 min, blocked with QuickBlock blocking buffer (Beyotime, China) for 30 min, and incubated with rabbit monoclonal c-Fos (9F6, 1:1000, Cell Signaling Technology, USA) and mouse monoclonal tyrosine hydroxylase (TH, F-11, 1:100, Santa Cruz) primary antibodies overnight at 4 °C. The next day, the sections were washed with phosphate buffered saline (PBS) and incubated with Alexa Fluor 594-conjugated AffiniPure Goat Anti-Rabbit IgG (H + L; 1:400, Jackson ImmunoResearch, USA) and fluorescein isothiocyanate-conjugated AffiniPure Goat Anti-Mouse IgG (H + L; 1:200, Jackson ImmunoResearch, USA) secondary antibodies for 2 h at room temperature. A confocal laser scanning microscope (Zeiss, Germany) was used to monitor the fluorescent signals.

2.7. Library preparation and sequencing

Following the standard rat atlas, the RVLM tissues were extracted by punching coronal sections [23]. cDNA libraries were generated as previously described [24]. In brief, TRIzol reagent (Invitrogen, USA) was utilized for the extraction of total RNA from RVLM tissues following the manufacturer's instructions. The purity and integrity of the RNA were evaluated using the NanoDrop ND-1000 (Thermo Scientific, USA) and 2100 Bioanalyzer System (Agilent, USA), respectively. Six high-quality cDNA libraries, which were designated as SIH (SIH_1, SIH_2, and SIH_3) and control (control_1, control_2, and control_3) groups, were constructed using the TruSeq Stranded Total RNA Human/Mouse/Rat kit (Illumina, USA) after the removal of ribosomal RNA by the Ribo-Zero rRNA Removal Kit (Illumina, USA). The libraries were tested for quality using the 2100 Bioanalyzer System (Agilent, USA). The resulting libraries were sequenced on an Illumina HiSeq 4000 instrument at Lianchuan Bio, generating 150 bp paired-end reads.

2.8. Analysis of differentially expressed circRNAs

Clean reads were obtained from raw data after filtering out reads with adaptors and low-quality and undetermined reads through Cutadapt [25]. The clean reads were then aligned to the rat genome (ftp://ftp.ensembl.org/pub/release-109/gtf/rattus_norvegicus/) using Bowtie2 and Hisat2 [26,27]. Tophat-fusion was used to further align the unmapped reads to the genome [28]. Back splicing reads were identified in the unmapped reads by CIRCExplorer2 [29]. All samples generated unique circRNAs. Differential expression analyses of circRNAs in the SIH and control groups were performed using edgeR [30]. p values < 0.05 were set as the filter criteria for significant differential expression of circRNAs.

2.9. Reverse transcription quantitative polymerase chain reaction (RT-qPCR)

The total RNAs were isolated from RVLM tissues or B104 cells as described above. The RNAs were reverse transcribed using Hifair II 1st Strand cDNA Synthesis Kit (Yeasen, China) in accordance with the manufacturer's specifications. A stem-loop RT primer (5′-GTCGTATCCAGTGCAGGGTCCGAGGTATTCGCACTGGATACGACACATTT-3′) was used for RT of miR-335. RT-qPCR was performed with 2 × Hieff qPCR SYBR Green Master Mix (Yeasen, China) on a CFX96 Touch Real-Time PCR Detection system (Bio-Rad, USA). Each 20 μL reaction volume contained 10 μL 2 × Hieff qPCR SYBR Green Master Mix (Yeasen, China), 7.2 μL PCR-grade H_2O, 2 μL cDNA template, and 0.4 μL of each 10 μM primer. The specific primers are shown in Table S1. GAPDH was used as the internal control for circRNA and mRNA normalization, and U6 was used for miR-335 normalization. Relative expression levels were calculated using the $2^{-\Delta\Delta Ct}$ method.

2.10. RT-PCR

The total RNAs were extracted from RVLM tissues and reverse transcribed to cDNA in accordance with the above procedure. RT-PCR was performed with 2 × Hieff PCR Master Mix (Yeasen, China) on a MyCycler Thermal Cycler system (Bio-Rad, USA). Each 25 μL reaction volume contained 12.5 μL 2 × Hieff PCR Master Mix (Yeasen, China), 8.5 μL PCR-grade H_2O, 2 μL cDNA template, and 1 μL of each 10 μM primer. The divergent and convergent primers of circRNA Galntl6 and the convergent primer of GAPDH used for RT-PCR are listed in Table S2. PCR products were detected by electrophoresis with 2% agarose gel or sequenced using Sanger sequencing.

2.11. RNase R treatment assay

The total RNAs were extracted from RVLM tissues as above and incubated with RNase R (Yeasen, China) at 37 °C for 30 min. The reaction volume contained 1 μg RNA, 0.2 μL RNase R (20 U/μL), and 2 μL 10 × RNase R Reaction Buffer. PCR-grade H_2O was then added to obtain a total volume of 20 μL. The RNAs treated with RNase R were purified using the RNeasy Mini Kit (QIAGEN, Germany) in accordance with the provided assay procedure. The purified RNAs were reverse transcribed to cDNA and then analyzed by RT-qPCR.

2.12. Fluorescence in-situ hybridization (FISH)

Cy3-labeled circRNA Galntl6 and negative control (NC) probes were synthesized by RiboBio (China). FISH was performed with a Fluorescent in Situ Hybridization Kit (RiboBio, China) in accordance with the manufacturer's manual. In brief, B104 cells were fixed at room temperature for 15 min with 4% paraformaldehyde. Then, the cells were permeabilized with 0.5% Triton X-100 at 4 °C for 5 min, blocked with prehybridization solution at 37 °C for 30 min, and incubated with a hybridization solution (circRNA Galntl6 probes or NC probes added) at 37 °C overnight in the dark. Afterward, the cells were stained with 4′,6-diamidino-2-phenylindole solution for 10 min in the dark. Finally, FISH images were analyzed by a confocal laser scanning microscope (Zeiss, Germany).

2.13. Nuclear and cytoplasmic fractionation

In accordance with the manufacturer's protocol, the RNAs from the nucleus and cytoplasm of B104 cells were separated and purified with a

Cytoplasmic & Nuclear RNA Purification Kit (Norgen Biotek, USA). The abundance of circRNA Galntl6 in cytoplasmic fraction or nuclear fraction was detected using RT-qPCR.

2.14. Intra-RVLM microinjection

The method of intra-RVLM microinjection has been described in the authors' previous studies [22,24]. In brief, the rats were anaesthetized with isoflurane as described above and placed in prone position, and their heads were fixed in a stereotaxic apparatus (RWD Life Science, China). A midline incision was made to expose the skull. The bregma and lambda points were aligned to the same horizontal plane. LV5 (EF-1a/GFP/Puro) > circRNA Galntl6 (pLV-circRNA Galntl6, lentiviral vector-mediated circRNA Galntl6 overexpression, > 10^9 TU/mL) and control LV5 (EF-1a/GFP/Puro) > NC (pLV-NC, > 10^9 TU/mL) plasmids were synthesized by GenePharma (China). A lentivirus containing shRNA targeting Lig3 (pLV-Lig3-shRNA) was constructed by Hanbio (China). As shown in Table S3, miR-335 agomir (1 nmol/μL), miR-335 antagomir (1 nmol/μL), and miR-335 antagomir NC (1 nmol/μL) were synthesized by GenePharma (China). In accordance with the rat brain atlas [23], they were microinjected into the bilateral RVLM (located 3.7–4.0 mm caudal to lambdoid suture, 2 mm lateral to the midline, and 8.0 mm ventral to the surface of the dura) of rats at 0.1 μL/side by a glass micropipette. The diagram used to demonstrate the process of confirming the correct positioning of RVLM was drawn and described in the authors' previous study [24]. The surgical incision was sutured after microinjection.

2.15. Cell transfection

The B104 cells were inoculated on culture plates and allowed to grow to 80% confluence. pLV-circRNA Galntl6 (GenePharma, China), pLV-NC (GenePharma, China), circRNA Galntl6 siRNA (si-circRNA Galntl6, Hanbio, China, Table S3), siRNA NC (si-NC, Hanbio, China, Table S3), miR-335 agomir (GenePharma, China, Table S3), agomir NC (GenePharma, China, Table S3), miR-335 antagomir (GenePharma, China, Table S3) and antagomir NC (GenePharma, China, Table S3) were transfected into B104 cells using Lipofectamine 8000 (Beyotime, China) following the manufacturer's instructions. After 48 h of transfection, the cells were utilized for subsequent analyses.

2.16. Detection of reactive oxygen species (ROS)

The ROS levels in RVLM were examined by the ROS-sensitive fluorescent dye dihydroethidium (DHE, Beyotime, China). RVLM sections were incubated with DHE (5 μM) for 30 min at 37 °C and washed thrice with PBS. Fluorescence was detected using a confocal laser scanning microscope (Zeiss, Germany).

2.17. Detection of 8-hydroxydeoxyguanosine (8-OH-dG)

A universal 8-OH-dG assay kit (FineTest, China) was used to measure 8-OH-dG following the manufacturer's instructions. In brief, the DNAs from RVLM tissues were isolated using a commercial extraction kit (Yeasen, China). Then, 50 μL DNA samples were added to the detection wells and incubated with 50 μL biotin-labeled antibody for 45 min at 37 °C, followed by incubation with 100 μL SABC working solution for 30 min at 37 °C. Subsequently, 90 μL TMB substrate was added to each well and incubated at 37 °C for 15 min. Finally, a stop solution was added, and the plate was read by the LabServ K3 microplate reader (Thermo Scientific, USA) at a wavelength of 450 nm.

2.18. Detection of superoxide dismutase (SOD) and catalase (CAT)

The enzymatic activities of SOD and CAT in RVLM were detected using commercially available assay kits (Beyotime, China) in accordance with the manufacturer's instructions. The absorbance was assessed at 450 and 520 nm by the LabServ K3 microplate reader (Thermo Scientific, USA). The SOD and CAT levels were normalized to the total protein.

2.19. Biotinylated RNA pull-down assay

Biotinylated miR-335 agomir (GenePharma, China) or biotinylated agomir NC (GenePharma, China) was transfected into the circRNA Galntl6-overexpressing B104 cells. The biotin-coupled RNA complex was pulled down by streptavidin magnetic beads (Thermo Scientific, USA). The amount of circRNA Galntl6 in the bound fraction was determined using RT-qPCR.

2.20. Dual-luciferase reporter assay

The potential wild-type (WT) and mutant (MUT) binding sites of miR-335 in circRNA Galntl6 sequence or Lig3 3′ UTR were synthesized and inserted into the pmirGLO dual-luciferase miRNA target expression vector to construct circRNA Galntl6-WT/MUT or Lig3-WT-3′ UTR/MUT-3′ UTR. The recombinant reporter plasmids and the miR-335 agomir (GenePharma, China) or agomir NC (GenePharma, China) were co-transfected into the B104 cells. A dual-luciferase reporter assay kit (Yeasen, China) was used to monitor the relative luciferase activity after 48 h following the manufacturer's protocol.

2.21. Western blot

The protein samples extracted from RVLM tissues or B104 cells were separated by 10% sodium dodecyl sulphate-polyacrylamide gel electrophoresis and transferred onto polyvinylidene difluoride membranes (Bio-Rad, USA). The membranes containing proteins were blocked with QuickBlock buffer (Beyotime, China) for 1 h at room temperature. Afterward, the membranes were blotted with rabbit polyclonal Lig3 (1:1000, ABclonal, China) and mouse monoclonal horseradish peroxidase (HRP)-conjugated GAPDH (1:5000, Proteintech, USA) primary antibodies at 4 °C overnight. After washing the membranes three times with PBST, they were hybridized with goat anti-rabbit IgG-HRP (1:3000, Cell Signaling Technology, USA) and horse anti-mouse IgG-HRP (1:3000, Cell Signaling Technology, USA) secondary antibodies for 1 h at room temperature. The signals of proteins were visualized using super ECL detection reagent (Yeasen, China) with the Tanon-5200 automatic chemiluminescence image analysis system (Tanon Science & Technology, China). GAPDH acted as a reference.

2.22. Statistical analysis

All values were shown as the mean ± standard error of the mean (SEM) and analyzed on GraphPad Prism software. The sample sizes used in this study were similar to those used in the authors' previous publications [24,31]. Unpaired two-tailed Student's *t*-test was employed to assess significant differences between two groups, and one-way ANOVA was used to analyze comparisons among three groups or more. The results were considered significant when $P < 0.05$.

3. Results

3.1. CircRNA Galntl6 was significantly lowly expressed in RVLM of SIH rats

After stress was stimulated for 15 successive days, the levels of BP, HR, sympathetic discharge, and RVLM neuronal excitability were investigated in SIH and control rats. A significant increase was found in the mean arterial pressure (MAP), HR, RSNA, plasma NE, and the number of c-Fos-positive TH + neurons of SIH rats compared with those of the control rats (Figs. S1A–D). These observations supported the

reliability of the SIH model. Next, the circRNA expression profiles in RVLM between the two groups were compared using RNA sequencing. 501,346,052 clean reads were obtained after sequencing and quality control, of which, 254,254,380 were from SIH group and 247,091,672 were from control group. A total of 12,242 circRNA transcripts were assembled and subjected to further analysis. The results showed that 32 circRNAs were differentially expressed at p value < 0.05. The top five differentially expressed circRNAs were marked by a heatmap (Fig. 1A). Further, RT-qPCR results demonstrated the excellent agreement of the expression patterns of three circRNAs (circRNA Galntl6, circRNA Acaca, and circRNA Sorbs1) with the RNA sequencing findings (Fig. 1B). CircRNA Adgrl3 and circRNA Pik3r1 did not show differential expression, which was inconsistent with the RNA sequencing data (Fig. S2). This finding was probably caused by biological differences between samples. The expression of circRNA Galntl6 in SIH rats dramatically decreased compared with that in the control rats (Fig. 1B), and it was

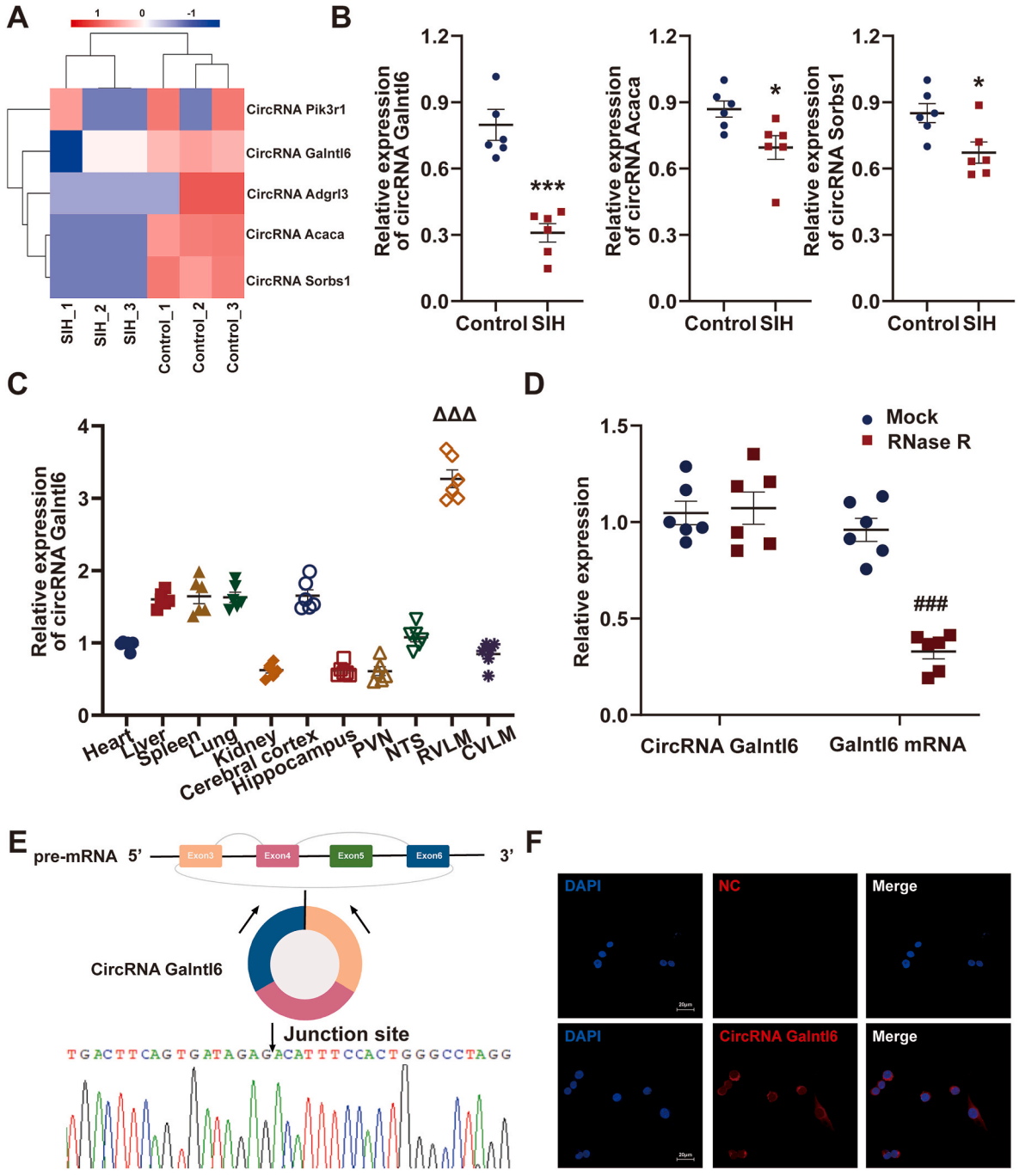

Fig. 1. CircRNA Galntl6 expression was downregulated in RVLM of SIH rats. (**A**) Heatmap shows the top five differentially expressed circRNAs identified by RNA sequencing between SIH and control rats. (**B**) RT-qPCR was used to measure the relative expressions of three indicated circRNAs listed in (A). (**C**) CircRNA Galntl6 expression was detected by RT-qPCR in 11 tissues of rats. (**D**) Expressions of circRNA Galntl6 and Galntl6 mRNA in RVLM tissues treated with or without RNase R were examined by RT-qPCR. (**E**) RT-PCR and Sanger sequencing were used to verify the existence of circRNA Galntl6. (**F**) FISH was performed to evaluate the subcellular localization of circRNA Galntl6 in B104 cells. Data were expressed as mean ± SEM. Statistical significance was determined by unpaired two-tailed Student's *t*-test (**B** and **D**) and one-way ANOVA, followed by post-hoc Bonferroni test (**C**). n = 6 rats per group (**B–D**). $^{*}p < 0.05$, $^{**}p < 0.01$ versus control group. $^{\Delta\Delta\Delta}p < 0.001$ versus heart group. $^{\#\#\#}p < 0.001$ versus mock group.

abundantly expressed in the RVLM tissue (Fig. 1C). Therefore, this study focused on the role of circRNA Galntl6 in SIH progression. When divergent and convergent primers were applied, circRNA Galntl6 was only amplified by divergent primers in cDNA, and no amplification product was detected in gDNA (Fig. S3). RNase R was used to confirm the stability of circRNA Galntl6. The results showed that circRNA Galntl6 was unaffected by RNase R, whereas Galntl6 mRNA was digested by it (Fig. 1D). Moreover, the head-to-tail splicing in the RT-PCR product of circRNA Galntl6 was verified through Sanger sequencing (Fig. 1E). The results of FISH and RT-qPCR revealed that circRNA Galntl6 was predominately located in the cytoplasm (Fig. 1F and Fig. S4); thus, it may perform its functions by acting as a competing endogenous RNA (ceRNA) to sponge its target miRNAs [32].

3.2. CircRNA Galntl6 overexpression in RVLM inhibited SIH progression

A gain-of-function system was established using pLV-circRNA Galntl6 to explore the biological functions of circRNA Galntl6 in SIH. The pLV-circRNA Galntl6 plasmid was bilaterally microinjected twice into the RVLM of rats in the SIH group 3 and 2 weeks before stress stimulation, respectively. The overexpression efficiency of circRNA Galntl6 in RVLM was verified using RT-qPCR (Fig. S5A). Radio telemetry demonstrated that the overexpression of circRNA Galntl6 significantly decreased the MAP and HR levels of SIH rats (Fig. 2A). Sympathetic outflow was then detected by RSNA recording test and plasma NE ELISA assay, and the results demonstrated that the RSNA and plasma NE values reduced dramatically after circRNA Galntl6 upregulation (Fig. 2B and C). The effect of circRNA Galntl6 on neuronal excitability was further revealed by immunofluorescence assay. The results displayed that circRNA Galntl6 overexpression markedly decreased the proportion of c-Fos-positive TH + neurons in the RVLM of SIH rats (Fig. 2D). The above results showed that circRNA Galntl6 can alleviate neuronal excitability, suppress sympathetic tone, and participate in the neurogenic regulation of SIH.

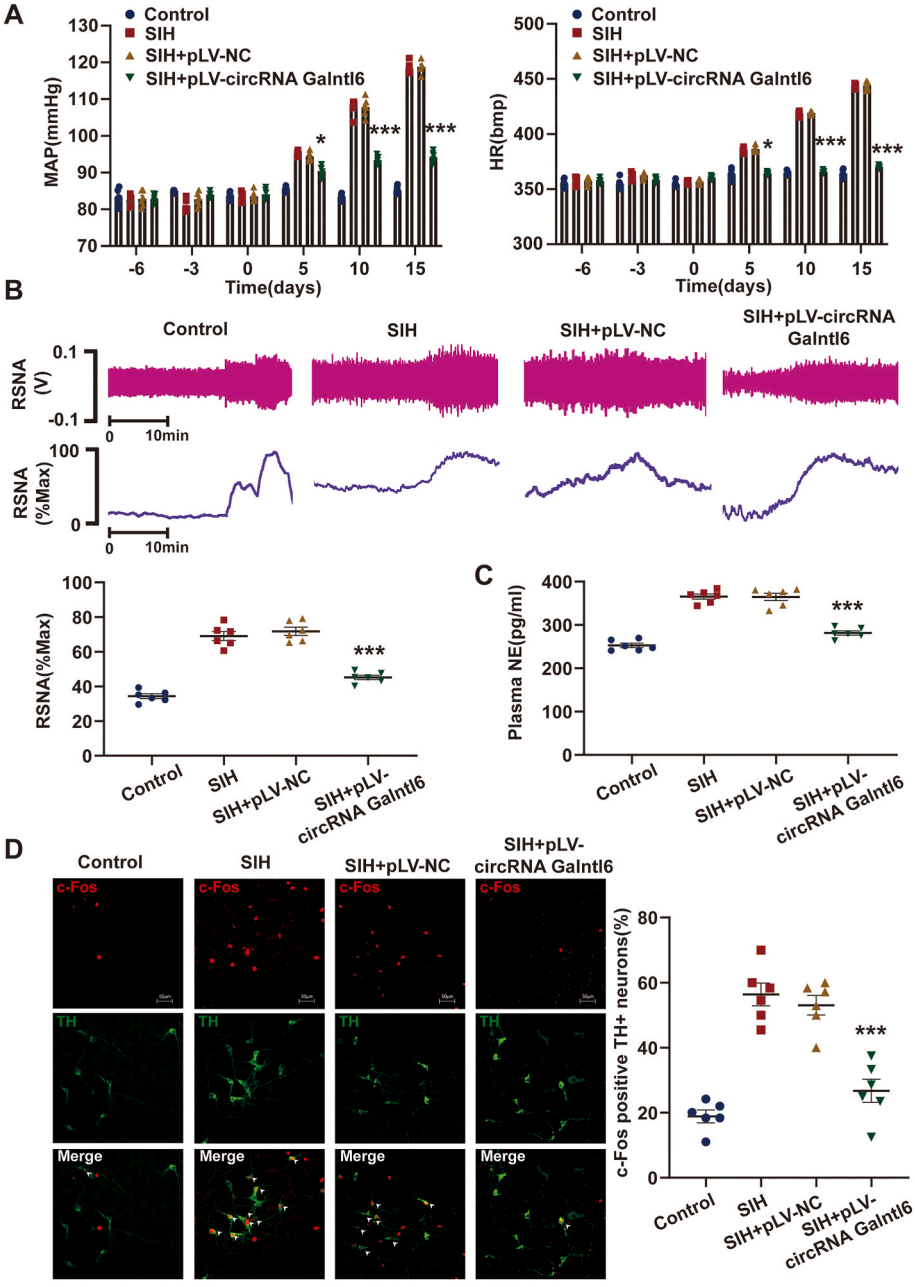

Fig. 2. Overexpression of circRNA Galntl6 in RVLM improved SIH. (**A**) Radio telemetry was used to measure the MAP and HR in rats after circRNA Galntl6 overexpression. (**B** and **C**) Effects of circRNA Galntl6 overexpression on the sympathetic outflow were unveiled using RSNA recording test and plasma NE ELISA. (**D**) RVLM neuronal excitability was detected by immunostaining with c-Fos. Data were expressed as mean ± SEM. Statistical significance was determined by one-way ANOVA, followed by post-hoc Bonferroni test (**A–D**). n = 6 rats per group (**A–D**). $^{*}p < 0.05$, $^{***}p < 0.001$, and ns means nonsignificant versus SIH group.

3.3. Upregulation of circRNA Galntl6 attenuated oxidative stress

Impaired oxidative stress in RVLM augments sympathetic vasomotor tone and contributes to hypertension [33–35]. The level of 8-OH-dG in RVLM was evaluated after pLV-circRNA Galntl6 plasmid was microinjected into the RVLM of SIH rats. The circRNA Galntl6 overexpression group exhibited a significant decrease in the level of 8-OH-dG (Fig. 3A). Fig. 3B and C showed that the upregulation of circRNA Galntl6 in RVLM observably increased the activities of SOD and CAT. Compared with that in the SIH and SIH + pLV-NC rats, ROS production in the RVLM of SIH + pLV-circRNA Galntl6 rat was markedly attenuated (Fig. 3D). These findings indicate that circRNA Galntl6 suppresses oxidative stress in RVLM to inhibit sympathetic hyperactivity against SIH.

3.4. CircRNA Galntl6 served as a sponge of miR-335

The underlying mechanism by which circRNA Galntl6 mediated oxidative stress was disclosed. Growing evidence has shown that circRNA-associated-ceRNA networks may have various functions in the regulation of numerous types of diseases [36,37]. We speculated that circRNA Galntl6 can bind to miRNAs to modulate downstream gene expressions because of its cytoplasmic localization. Our previous studies revealed that knockdown of miR-335 in RVLM significantly reduced sympathetic outflow and effectively improved SIH [24,31]. In the present study, the results of RT-qPCR showed that miR-335 expression was upregulated in the RVLM of SIH rats (Fig. S6). Bioinformatics prediction by RNAhybrid showed the binding sites of miR-335 in circRNA Galntl6 (Fig. 4A). Biotinylated miR-335 agomir or biotinylated agomir NC was utilized to pull down circRNA Galntl6 in B104 cells with circRNA Galntl6 overexpression, and the results revealed that circRNA Galntl6 was mainly abundant in the biotinylated miR-335 agomir group (Fig. 4B). Next, reporter assay was conducted with a luciferase plasmid harboring the circRNA Galntl6 sequence containing the predicted sites of miR-335. As shown in Fig. 4C, the luciferase activity of circRNA Galntl6-WT was dramatically decreased by miR-335 overexpression. However, the luciferase activity of circRNA Galntl6-MUT had no evident change. In addition, the circRNA Galntl6 expression was overexpressed or inhibited efficiently in the B104 cells (Figs. S5B–C), and the results showed that overexpression or knockdown of circRNA Galntl6 could negatively regulate the expression of miR-335 (Fig. 4D and E). This regulatory relationship was further verified in-vivo, and the results indicated that the circRNA Galntl6 overexpression in RVLM markedly decreased the miR-335 expression (Fig. 4F). The above results proved that circRNA Galntl6 can directly sponge miR-335.

3.5. CircRNA Galntl6 restrained oxidative stress by absorbing miR-335

Whether circRNA Galntl6 regulates oxidative stress through sponging miR-335 was further revealed. The pLV-circRNA Galntl6 plasmid was bilaterally microinjected twice into the RVLM of rats in the SIH group 3 and 2 weeks before stress stimulation, respectively. Then, the rats were administered with two bilateral RVLM microinjections of miR-335 agomir on days 8 and 12 of stress. The levels of oxidative stress in the groups were detected on day 15 of stress. MiR-335 agomir

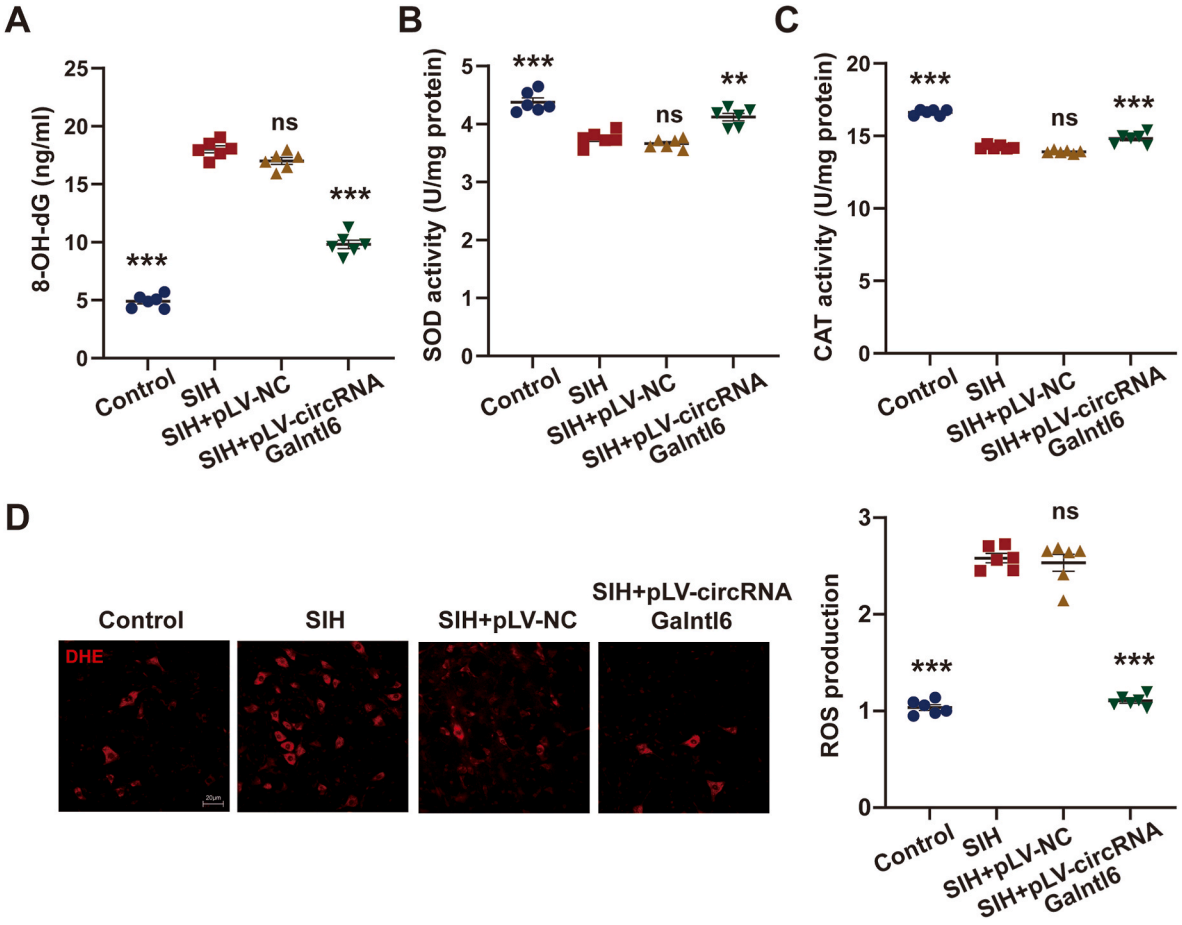

Fig. 3. CircRNA Galntl6 restricted RVLM oxidative stress in SIH rats. (**A–D**) After microinjection of pLV-circRNA Galntl6 plasmid in the RVLM of SIH rats, the level of 8-OH-dG and the activities of SOD and CAT were determined by commercial kits, and ROS production was detected by DHE staining. Data were expressed as mean ± SEM. Statistical significance was determined by one-way ANOVA, followed by post-hoc Bonferroni test (**A–D**). n = 6 rats per group (**A–D**). *$p < 0.05$, ***$p < 0.001$, and ns means nonsignificant versus SIH group.

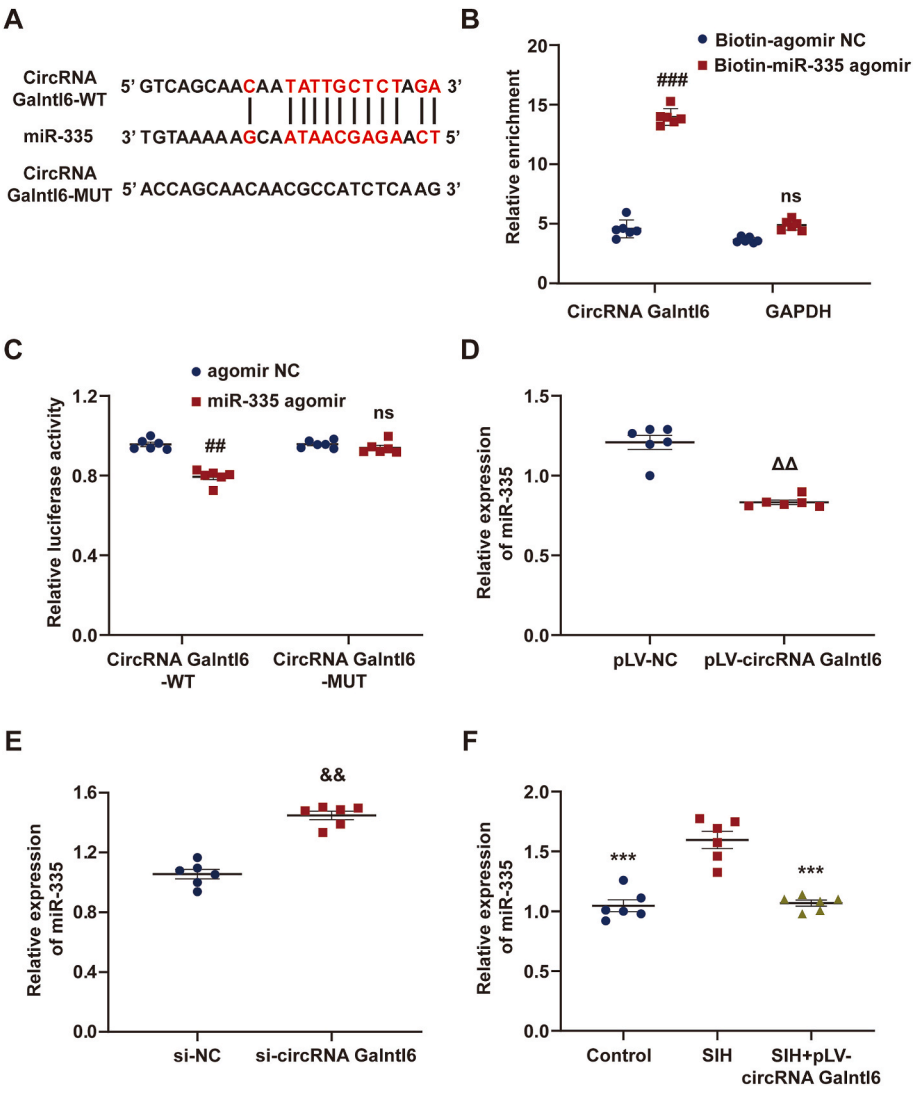

Fig. 4. CircRNA Galntl6 bound to miR-335 and decreased its expression. (**A**) Predicted binding sites between circRNA Galntl6 and miR-335. (**B**) RNA pulldown assay showed that biotin-labeled miR-335 interacted with circRNA Galntl6. (**C**) Dual-luciferase reporter assay was used to confirm the targeted relationship between circRNA Galntl6 and miR-335. (**D** and **E**) RT-qPCR was used to measure the effect of circRNA Galntl6 overexpression or knockdown on miR-335 expression in B104 cells. (**F**) Relative expression of miR-335 was detected by RT-qPCR in RVLM administrated with pLV-circRNA Galntl6 plasmid. Data were expressed as mean ± SEM. Statistical significance was determined by unpaired two-tailed Student's *t*-test (**B–E**) and one-way ANOVA, followed by post-hoc Bonferroni test (**F**). n = 6 of independent cell culture preparations (**B–E**). n = 6 rats per group (**F**). $^{\#\#}p < 0.01$, $^{\#\#\#}p < 0.001$, and ns means nonsignificant versus agomir NC group. $^{\Delta\Delta}p < 0.01$ versus pLV-NC group. $^{\&\&}p < 0.01$ versus si-NC group. $^{**}p < 0.01$, and ns means nonsignificant versus SIH group.

attenuated the suppressive effects of circRNA Galntl6 overexpression on the level of 8-OH-dG in the RVLM of SIH rats (Fig. 5A). The promotive influence of circRNA Galntl6 overexpression on the activities of SOD and CAT was reversed after microinjection of miR-335 agomir into RVLM (Fig. 5B and C). Moreover, miR-335 agomir impaired the inhibitory effects of circRNA Galntl6 overexpression on the ROS production in the RVLM of SIH rats (Fig. 5D). Overall, these results indicate that circRNA Galntl6 regulates miR-335 to affect oxidative stress in RVLM, which participates in SIH pathogenesis.

3.6. *Lig3 was a direct target of miR-335*

The mechanism underlying miR-335 modulating oxidative stress was unveiled. Lig3 is critical for mitochondrial DNA integrity, and it strongly affects oxidative stress [38–40]. In the present study, the expression of Lig3 in RVLM was examined by RT-qPCR and Western blot in SIH and control rats, and the results showed that the mRNA and protein expression levels of Lig3 in SIH rats greatly decreased (Fig. S7). MiR-335 may target Lig3 directly, as predicted by the TargetScan and miRanda tools (Fig. 6A). The results of dual-luciferase reporter assay confirmed that the upregulation of miR-335 by agomir in B104 cells observably decreased the luciferase activity of Lig3-WT-3′ UTR reporter, whereas it had no remarkable effect on the Lig3-MUT-3′ UTR reporter (Fig. 6B). Then, miR-335 overexpression and knockdown systems were established successfully in B104 cells using miR-335 agomir and miR-335 antagomir, and the overexpression and knockdown efficiencies were detected by RT-qPCR (Figs. S5D–E). As shown in Fig. 6C, the mRNA and protein levels of Lig3 dramatically decreased when miR-335 was overexpressed. By contrast, miR-335 knockdown led to a significant increase in Lig3 expression (Fig. 6D). For in-vivo assay, the miR-335 antagomir was bilaterally microinjected into the RVLM of rats in the SIH group on days 8 and 12 of stress. This regulatory relationship was measured on day 15 of stress. RT-qPCR was used to evaluate the knockdown efficiency of miR-335 antagomir in RVLM (Fig. S5F). The results revealed that miR-335 downregulation in RVLM observably increased the Lig3 expression (Fig. 6E). Altogether, these observations prove that miR-335 targets Lig3.

3.7. *MiR-335 promoted oxidative stress by targeting Lig3*

Given the binding relationship between miR-335 and Lig3, the effect of miR-335/Lig3 on oxidative stress was clarified. The pLV-Lig3-shRNA plasmid was bilaterally microinjected twice into the RVLM of rats in the SIH group 3 and 2 weeks before stress stimulation, respectively. The rats were then administered with two bilateral RVLM microinjections of miR-335 antagomir on days 8 and 12 of stress. The oxidative stress levels in the groups were examined on day 15 of stress. As shown in Fig. 7A, miR-335 knockdown reduced the level of 8-OH-dG in the RVLM of SIH

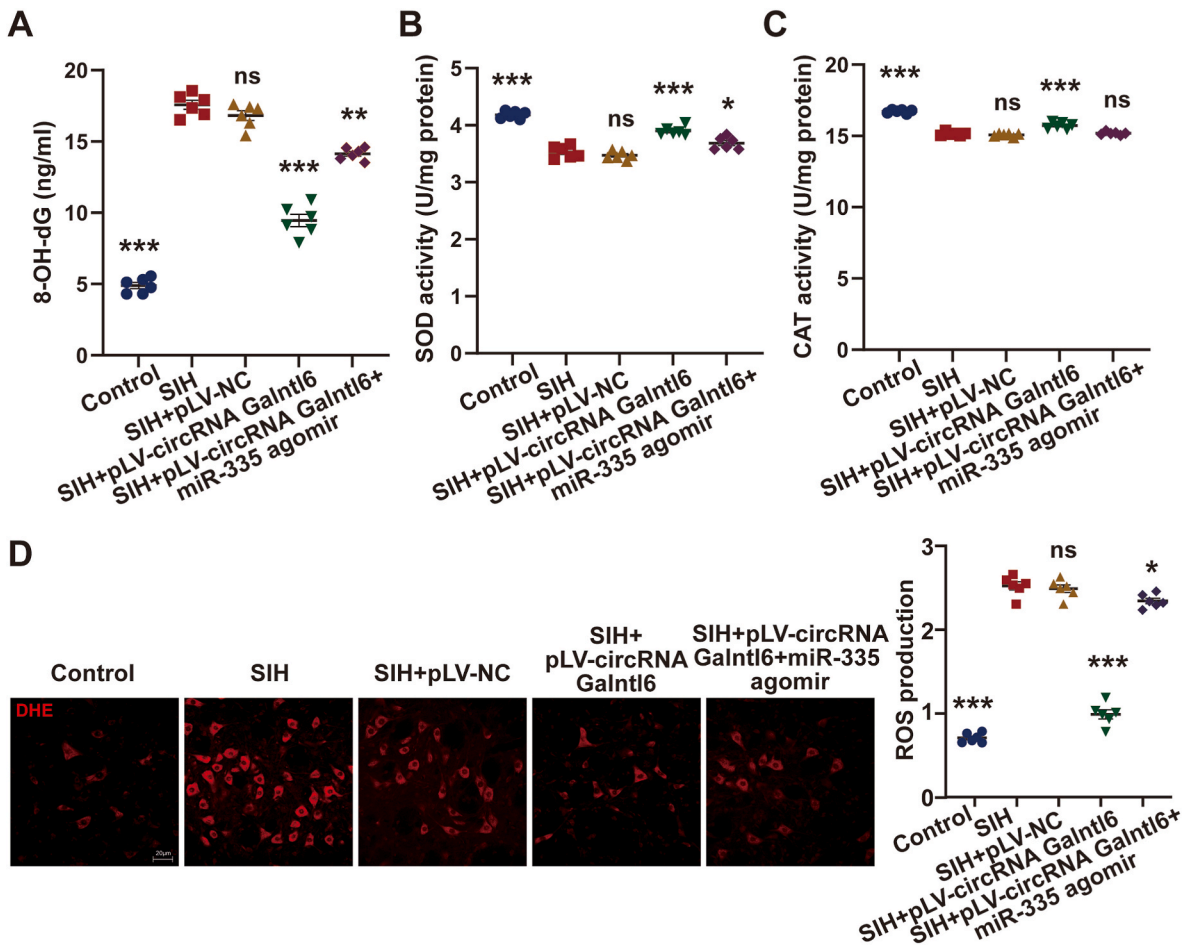

Fig. 5. CircRNA Galntl6 repressed oxidative stress in RVLM of SIH rats by binding to miR-335. (**A–C**) Effects of circRNA Galntl6 overexpression and miR-335 agomir on the level of 8-OH-dG and activities of SOD and CAT in RVLM were measured using commercial kits. (**D**) Influences of circRNA Galntl6 upregulation and miR-335 agomir on ROS production in RVLM were detected by DHE staining. Data were expressed as mean ± SEM. Statistical significance was determined by one-way ANOVA, followed by post-hoc Bonferroni test (**A–D**). n = 6 rats per group (**A–D**). $^{*}p < 0.05$, $^{**}p < 0.01$, $^{***}p < 0.001$, and ns means nonsignificant versus SIH group.

rats, whereas enforced Lig3 inhibition attenuated this influence. MiR-335 downregulation increased the activities of SOD and CAT in the RVLM of SIH rats, which were restored after Lig3 suppression (Fig. 7B and C). ROS production in the RVLM of SIH rats was decreased by miR-335 antagomir. However, Lig3 knockdown hindered this effect (Fig. 7D). Collectively, these findings suggest that miR-335 regulates oxidative stress in RVLM by targeting Lig3 and plays a key role in SIH progression.

3.8. CircRNA Galntl6 modulated Lig3 expression by targeting miR-335

MiR-335 was confirmed to be sponged by circRNA Galntl6, and Lig3 was a target of miR-335. Thus, whether circRNA Galntl6 regulates Lig3 expression by targeting miR-335 was further uncovered. RT-qPCR and Western blot analyses revealed that the mRNA and protein levels of Lig3 were observably upregulated or downregulated by circRNA Galntl6 overexpression or silencing in B104 cells, whereas miR-335 agomir or antagomir reversed these effects (Fig. 8A–D). In-vivo assay showed the significantly increased expression of Lig3 in the RVLM of SIH + pLV-circRNA Galntl6 rats. However, miR-335 agomir administration notably prevented this increase (Fig. 8E and F). To sum up, these data prove that circRNA Galntl6 can modulate the expression of Lig3 through sponging miR-335.

4. Discussion

CircRNAs were first described in 1976 in plant viroids [41]. Afterward, research has increasingly uncovered their generation and expression in humans, animals, and plants. Given the widespread existence of circRNAs, they have been well evaluated and were abnormal under disease conditions [42]. However, no relevant studies have identified the association between circRNAs and the neurogenic pathogenesis of hypertension. RVLM is a unique and important brain region involved in the control of sympathetic discharge and hypertension [11, 43]. Here, the first comprehensive and dynamic genome-wide RVLM circRNA catalog in SIH rats and controls was successfully built, which revealed their functional roles in modulating SIH progression and great potential as therapeutic targets.

In general, altered expression can help in verifying the different biological processes between healthy and abnormal states. In-silico analysis of the circRNAs in RVLM showed that showed that 19 circRNAs were upregulated, and 13 were downregulated in response to stress. CircRNA Galntl6, a RVLM-enriched circRNA, was poorly expressed in SIH rats, as further recognized by RT-qPCR. CircRNA Galntl6 is an exonic circRNA that originates from exons 3, 4, and 6 of the Galntl6 gene and is then back spliced into a circular structure. In-vivo comes from the Latin (within the living), meaning a study is performed on a living organism. In-vivo studies display high accuracy in the validation of targets and are important in novel therapy development. Lentivirus-mediated overexpression of circRNA Galntl6 in-vivo markedly reduced the

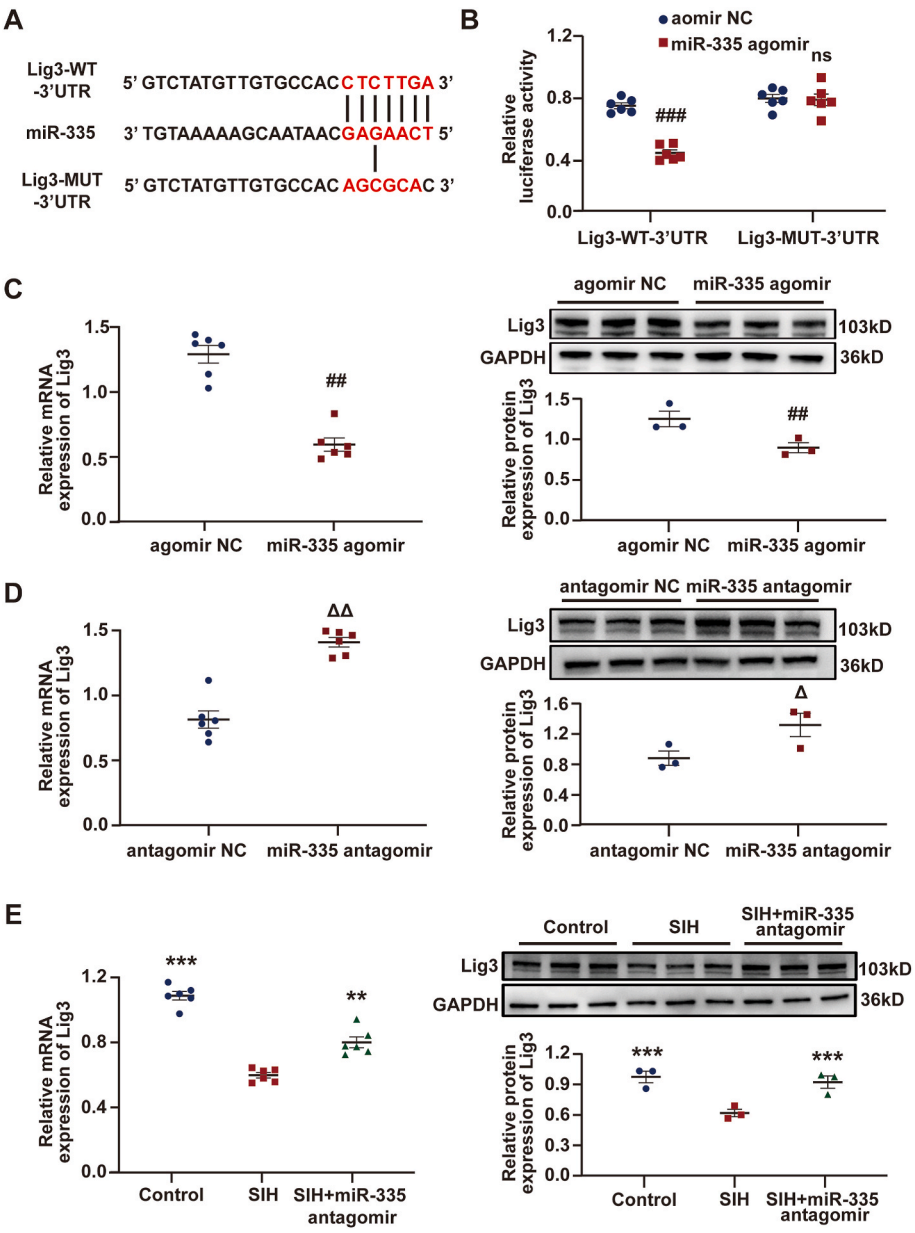

Fig. 6. Lig3 was a downstream mRNA target of miR-335. (**A**) Schematic graph of the potential binding sites for miR-335 within Lig3 3′ UTR. (**B**) The luciferase activities of Lig3 luciferase reporters (WT or MUT) were tested in B104 cells co-expressing miR-335 agomir or agomir NC. (**C** and **D**) RT-qPCR and Western blot analyses showed that the expression of Lig3 decreased or increased in B104 cells when miR-335 was overexpressed or downregulated, respectively. (**E**) Following miR-335 knockdown in RVLM of SIH rats, Lig3 expression was measured using RT-qPCR and Western blot assays. Data were expressed as mean ± SEM. Statistical significance was determined by unpaired two-tailed Student's *t*-test (**B–D**) and one-way ANOVA, followed by post-hoc Bonferroni test (**E**). n = 3–6 of independent cell culture preparations (**B–D**). n = 3–6 rats per group (**E**). $^{\#\#}p < 0.01$, $^{\#\#\#}p < 0.001$, and ns means nonsignificant versus agomir NC group. $^{\Delta}p < 0.05$, and $^{\Delta\Delta}p < 0.01$ versus antagomir NC group. $^{**}p < 0.01$, and $^{***}p < 0.001$ versus SIH group.

levels of MAP, HR, RSNA, and plasma NE and the percentage of RVLM TH + neurons expressing c-Fos. Therefore, the data establish circRNA Galntl6 as an essential ncRNA in the regulation of BP, sympathetic outflow, and RVLM neuronal excitability during the progression of SIH.

Reportedly, oxidative stress in the cardiovascular center plays an important part in the regulation of sympathetic outflow in hypertension [44]. Mounting evidence showed that oxidative stress in RVLM can increase sympathetic nerve activity, which leads to hypertension [33–35]. In the present study, upregulated circRNA Galntl6 can reduce the 8-OH-dG level, MMP depolarization, and ROS production and enhance SOD and CAT activities in-vivo, which suggest that circRNA Galntl6 inhibited RVLM oxidative stress to hinder the course of SIH. The biological functions of circRNAs heavily rely upon their subcellular localization [16]. Cytoplasmic circRNAs can modulate mRNA stability via acting as miRNA sponges [32]. FISH and cytoplasmic and nuclear RT-qPCR assays revealed that circRNA Galntl6 was mainly located in the cytoplasm. Given that circRNA Galntl6 may serve as a sponge of miRNAs to regulate RVLM oxidative stress and SIH progression, miRNAs associated with circRNA Galntl6 were further sought.

MiR-335, an evolutionarily conserved miRNA in humans, mice, rats, and other species, is involved in the regulation of various pathological processes. Li et al. uncovered that miR-335 exacerbated type 2 diabetes through inhibiting the expression of SLC2A4 [45]. MiR-335 targeted HMG-box transcription factor 1 to promote chondrocyte apoptosis in osteoarthritis [46]. Moreover, miR-335 has been implicated in various aspects of tumor progression [47]. Importantly, miR-335 was positively associated with oxidative stress [48,49]. The authors' previous studies revealed that miR-335 silencing in RVLM repressed SIH progression via regulating sympathetic vasoconstriction [24,31]. Herein, miR-335 was dramatically upregulated in the RVLM of SIH rats compared with the controls. Using RNA pulldown, dual-luciferase reporter, gain-of-function, and loss-of-function analyses, circRNA Galntl6 was demonstrated to directly target and suppress miR-335 expression. Furthermore, miR-335 agomir attenuated the circRNA Galntl6-mediated effects on oxidative stress in-vivo. These findings prove that circRNA Galntl6 regulates RVLM oxidative stress by sponging miR-335, which participates in SIH pathogenesis.

Next, the downstream gene of miR-335 and the molecular

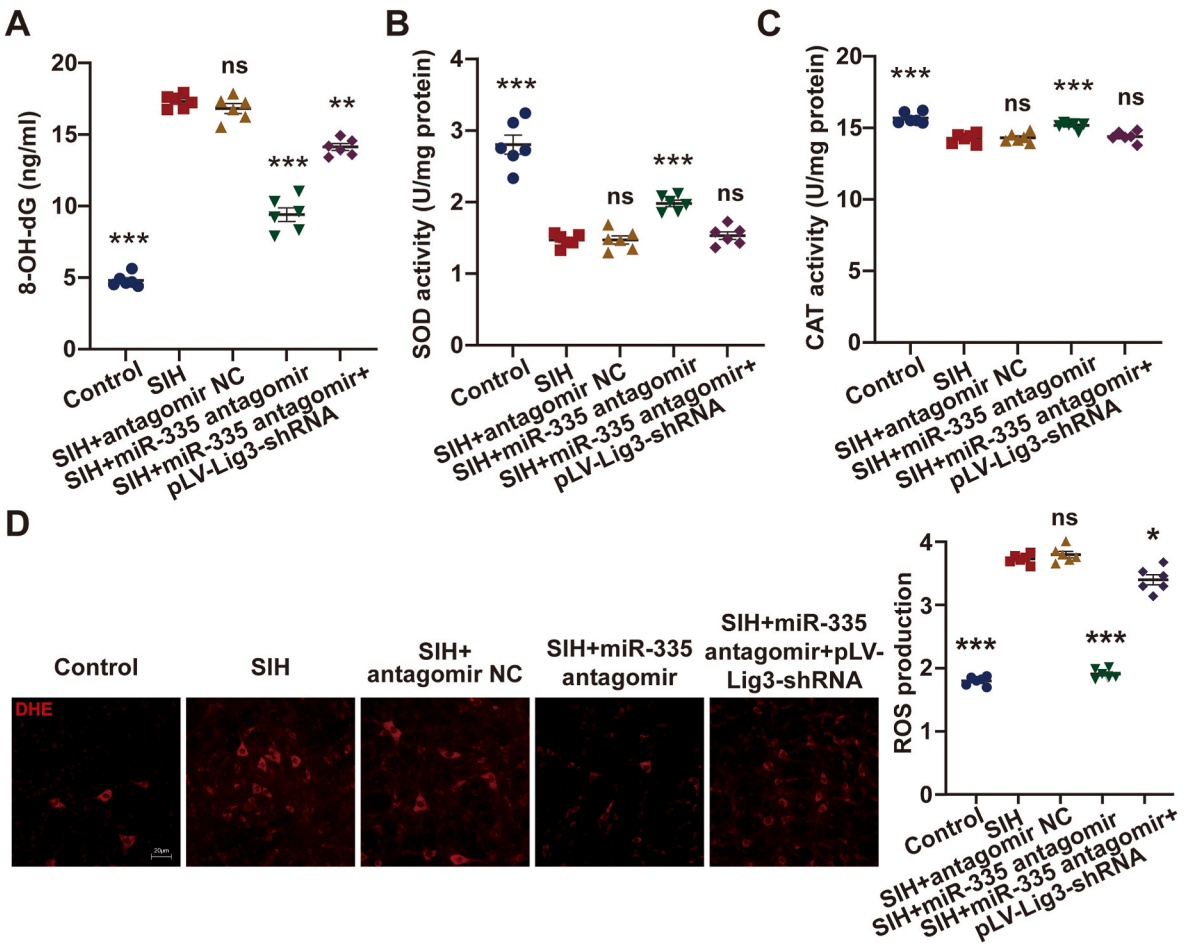

Fig. 7. MiR-335 caused oxidative stress in RVLM of SIH rats via targeting Lig3. (**A–C**) Effects of miR-335 downregulation on the level of 8-OH-dG and activities of SOD and CAT in RVLM of SIH rats were reversed by Lig3 depletion. (**D**) Lig3 knockdown weakened the suppressive influence of miR-335 silencing on ROS production in RVLM of SIH rats. Data were expressed as mean ± SEM. Statistical significance was determined by one-way ANOVA, followed by post-hoc Bonferroni test (**A–D**). n = 6 rats per group (**A–D**). $^{*}p < 0.05$, $^{**}p < 0.01$, $^{***}p < 0.001$, and ns means nonsignificant versus SIH group.

mechanism of how miR-335 perform its role in SIH progression were explored. Mature miRNA was loaded onto AGO to assemble RNA-induced silencing complex, which then mediates gene silencing activities [50]. DNA ligase 3, which is encoded by Lig3, is the only DNA ligase detected in mitochondria, and it exerts an antioxidative stress effect [38–40]. In the current study, Lig3 was down-expressed in the RVLM of SIH rats and negatively correlated with miR-335 expression. Dual-luciferase reporter, gain-of-function, and loss-of-function assays revealed that Lig3 is a direct target of miR-335. In addition, Lig3 suppression reversed the effects of miR-335 antagomir on oxidative stress in-vivo. The above data proved that miR-335 modulates RVLM oxidative stress via targeting Lig3, which further affects SIH progression.

In addition, in-vivo and in-vitro experiments were employed to disclose the relationship between circRNA Galntl6 and Lig3. The overexpression of circRNA Galntl6 enhanced Lig3 expression, whereas knockdown of circRNA Galntl6 reduced it. However, these effects were restrained by miR-335 agomir or antagomir. All these findings suggest that circRNA Galntl6 can sponge miR-335 to regulate Lig3 expression. CircRNA Galntl6 inhibits SIH progression by controlling RVLM oxidative stress, and the underlying molecular mechanism is that circRNA Galntl6 promotes Lig3 expression by targeting miR-335. However, this research has some limitations. First, BP is profoundly affected by sex difference [51], and in the present study, only male rat samples were used. Second, more experiments are needed to detect other target genes and signals in the RVLM involved in circRNA Galntl6-mediated SIH progression. Lastly, the expression of circRNA Galntl6 in other cardiovascular centers (NTS and CVLM) and the associated mechanisms should be explored intensively. Moreover, the renin-angiotensin-aldosterone system (RAS) plays a crucial role in the physiologic regulation of pressor response [52]. Enhanced excitability of RVLM neurons causes elevated sympathetic nerve activity (SNA) and increases plasma renin and angiotensin II levels [53]. Circulating angiotensin II increases neuronal activity in the subfornical organ (SFO), and this increased activity is relayed to the paraventricular nucleus (PVN) and subsequently to the RVLM, contributing to the maintenance of RVLM neuron activities, which accentuates SNA and hypertension [53,54]. In the present study, circRNA Galntl6 overexpression in RVLM dramatically reduced the sympathetic tone. Thus, we speculated that circRNA Galnt6 can also modulate the RAS to fight against SIH.

Chronic stress has an effect on the neuronal excitability of cardiovascular centers, which can place people at serious risk of SIH. It augments the excitation of RVLM neurons and sympathetic nerve activity to induce SIH. Rat models of SIH established by long-term electric footshock stimulation and buzzer noise exposure are considered reliable models for studying the pathological changes in SIH [12–14,22,24,31]. The present study depicted a comprehensive view of RVLM circRNA transcriptome in SIH rats and the discovery of a novel regulatory mechanism of circRNA Galntl6 that controls RVLM oxidative stress and neuronal excitability, sympathetic outflow, and BP. Mechanistically, circRNA Galntl6 can effectively sponge miR-335 to promote Lig3 expression in RVLM. These findings suggest targeting the circRNA Galntl6/miR-335/Lig3 axis as an effective treatment strategy for

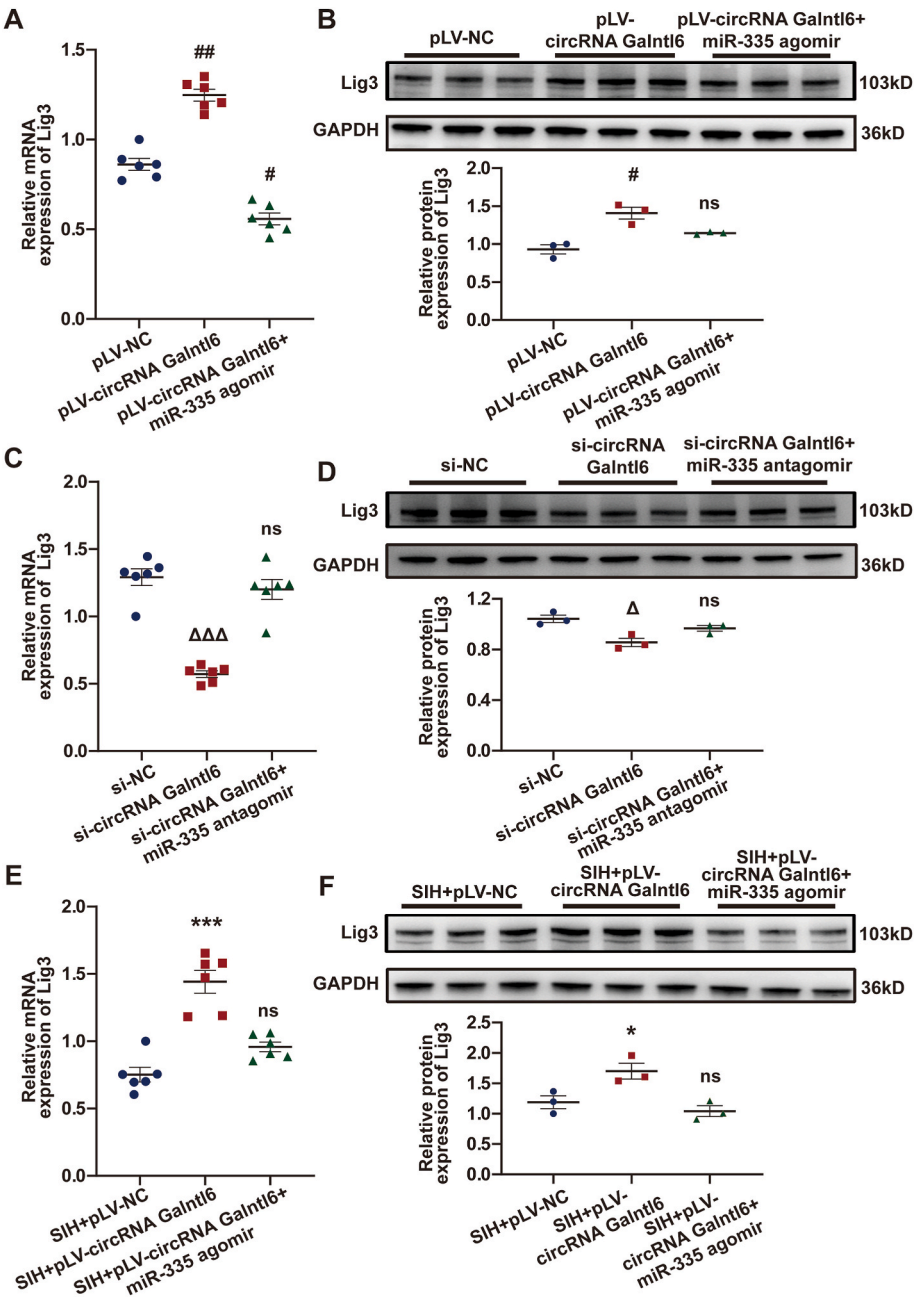

Fig. 8. CircRNA Galntl6 regulated Lig3 expression via targeting miR-335. (**A** and **B**) Effects of circRNA Galntl6 overexpression and miR-335 agomir on the expression of Lig3 were revealed using RT-qPCR and Western blot analyses in B104 cells. (**C** and **D**) RT-qPCR and Western blot assays were used to illustrate the effects of circRNA Galntl6 knockdown and miR-335 antagomir on Lig3 expression in B104 cells. (**E** and **F**) After microinjection of pLV-circRNA Galntl6 plasmid and miR-335 agomir into RVLM of SIH rats, the expression of Lig3 was measured by RT-qPCR and Western blot analyses. Data were expressed as mean ± SEM. Statistical significance was determined by one-way ANOVA, followed by post-hoc Bonferroni test (**A–F**). n = 6 of independent cell culture preparations (**A** and **C**). n = 3 of independent cell culture preparations (**B** and **D**). n = 6 rats per group (**E**). n = 3 rats per group (**F**). $^{\#}p < 0.05$, $^{\#\#}p < 0.001$, and ns means nonsignificant versus pLV-NC group. $^{\Delta}p < 0.05$, $^{\Delta\Delta\Delta}p < 0.001$, and ns means nonsignificant versus si-NC group. $^{*}p < 0.05$, $^{***}p < 0.001$, and ns means nonsignificant versus SIH + pLV-NC group.

combatting SIH.

Funding

This study was supported by the National Natural Science Foundation of China (32071111, 31871151, 31571171 and 32200929), the Natural Science Foundation of Shandong Province (ZR202112030301), the Special project of Science and Technology Plan of Shaoxing Bureau of Science and Technology (2020B33004), and the Zhejiang Chinese Medical University Research Funding (111100E018/002/001/077 and 111100E018/002/001/096).

Author contributions

S.Z. and D.D.S. were responsible for acquisition of funding. S.Z. and D.D.S. contributed to the design of the research. S.Z., X.P.W, G.J.C., L.T., T.T.D., L.P.W., and H.L.Z. performed the experiments. S.Z., X.P.W, G.J.C., and L.C.Z. contributed to the data analysis. S.Z. wrote the manuscript. All authors read and approved the final manuscript.

Declaration of competing interest

The authors declare no conflicts of interest.

Data availability

Data will be made available on request.

Acknowledgments

We thank Mr. Chao Jiang at Lianchuan Bio for his assistance.

Appendix A. Supplementary data

Supplementary data to this article can be found online at https://doi.org/10.1016/j.redox.2023.102782.

References

[1] S. Mennuni, S. Rubattu, G. Pierelli, G. Tocci, C. Fofi, M. Volpe, Hypertension and kidneys: unraveling complex molecular mechanisms underlying hypertensive renal damage, J. Hum. Hypertens. 28 (2014) 74–79.
[2] J.G. Yu, R.R. Zhou, G.J. Cai, From hypertension to stroke: mechanisms and potential prevention strategies, CNS Neurosci. Ther. 17 (2011) 577–584.
[3] K.T. Mills, A. Stefanescu, J. He, The global epidemiology of hypertension, Nat. Rev. Nephrol. 16 (2020) 223–237.
[4] P.M. Kearney, M. Whelton, K. Reynolds, P. Muntner, P.K. Whelton, J. He, Global burden of hypertension: analysis of worldwide data, Lancet 365 (2005) 217–223.
[5] P. Rust, C. Ekmekcioglu, Impact of salt intake on the pathogenesis and treatment of hypertension, Adv. Exp. Med. Biol. 956 (2017) 61–84.
[6] M.Y. Liu, N. Li, W.A. Li, H. Khan, Association between psychosocial stress and hypertension: a systematic review and meta-analysis, Neurol. Res. 39 (2017) 573–580.
[7] J.L. Boone, Stress and hypertension, Prim Care 18 (1991) 623–649.
[8] G. Mancia, G. Grassi, The autonomic nervous system and hypertension, Circ. Res. 114 (2014) 1804–1814.
[9] D. Hering, K. Lachowska, M. Schlaich, Role of the sympathetic nervous system in stress-mediated cardiovascular disease, Curr. Hypertens. Rep. 17 (2015) 80.
[10] E. Colombari, M.A. Sato, S.L. Cravo, C.T. Bergamaschi, R.R. Campos Jr., O. U. Lopes, Role of the medulla oblongata in hypertension, Hypertension 38 (2001) 549–554.
[11] P.G. Guyenet, R.L. Stornetta, B.B. Holloway, G.M.P.R. Souza, S.B.G. Abbott, Rostral ventrolateral medulla and hypertension, Hypertension 72 (2018) 559–566.
[12] K. Ooi, L. Hu, Y. Feng, C.Z. Han, X.R. Ren, X.Y. Qian, H.F. Huang, S.J. Chen, Q. Shi, H. Lin, et al., Sigma-1 receptor activation suppresses microglia M1 polarization via regulating endoplasmic reticulum-mitochondria contact and mitochondrial functions in stress-induced hypertension rats, Mol. Neurobiol. 58 (2021) 6625–6646.
[13] H.Y. Yang, X.S. Song, Z.M. Wei, C.M. Xia, J.J. Wang, L.L. Shen, J. Wang, TLR4/MyD88/NF-κB signaling in the rostral ventrolateral medulla is involved in the depressor effect of candesartan in stress-induced hypertensive rats, ACS Chem. Neurosci. 11 (2020) 2978–2988.
[14] J.X. Wu, L. Tong, L. Hu, C.M. Xia, M. Li, Q.H. Chen, F.X. Chen, D.S. Du, Upregulation of Nav1.6 expression in the rostral ventrolateral medulla of stress-induced hypertensive rats, Hypertens. Res. 41 (2018) 1013–1022.
[15] P.J. Zhang, W.Y. Wu, Q. Chen, M. Chen, Non-coding RNAs and their integrated networks, J Integr Bioinform 16 (2019), 20190027.
[16] C.X. Liu, L.L. Chen, Circular RNAs: characterization, cellular roles, and applications, Cell 185 (2022) 2016–2034.
[17] L. Farkas, E.A. Goncharova, Circling in on pulmonary arterial hypertension: is it time to consider circular RNA circ_0016070 as a biomarker and target for therapy? J. Am. Heart Assoc. 11 (2022), e026798.
[18] X.G. Jing, S.J. Wu, Y. Liu, H. Wang, Q.F. Huang, Circular RNA Sirtuin1 represses pulmonary artery smooth muscle cell proliferation, migration and autophagy to ameliorate pulmonary hypertension via targeting microRNA-145-5p/protein kinase-B3 axis, Bioengineered 13 (2022) 8759–8771.
[19] S.Y. Zheng, T.L. Gu, X.J. Bao, J.H. Sun, J.S. Zhao, T. Zhang, L.N. Zhang, Circular RNA hsa_circ_0014243 may serve as a diagnostic biomarker for essential hypertension, Exp. Ther. Med. 17 (2019) 1728–1736.
[20] National Research Council (US) Institute for Laboratory Animal Research, Guide for the Care and Use of Laboratory Animals, National Academies Press, 1996.
[21] National Research Council (US), Committee for the Update of the Guide for the Care and Use of Laboratory Animals. Guide for the Care and Use of Laboratory Animals, National Academies Press, 2011.
[22] L. Tong, M.Y. Xing, J.X. Wu, S. Zhang, D.C. Chu, H.L. Zhang, F.X. Chen, D.S. Du, Overexpression of NaV1.6 in the rostral ventrolateral medulla in rats mediates stress-induced hypertension via glutamate regulation, Clin. Exp. Hypertens. 44 (2022) 134–145.
[23] G. Paxinos, C. Watson, Paxinos and Watson's the Rat Brain in Stereotaxic coordinates, Academic Press, 2014.
[24] S. Zhang, G.J. Chen, X.P. Wang, L. Tong, L.P. Wang, T.F. Liu, L.C. Zhu, S.M. Zhou, H.S. Liu, D.S. Du, LncRNA INPP5F ameliorates stress-induced hypertension via the miR-335/Cttn axis in rostral ventrolateral medulla, CNS Neurosci. Ther. (2023).
[25] M. Martin, Cutadapt removes adapter sequences from high-throughput sequencing reads, EMBnet Journal 17 (2011) 10–12.
[26] B. Langmead, S.L. Salzberg, Fast gapped-read alignment with Bowtie2, Nat. Methods 9 (2012) 357–359.
[27] D. Kim, B. Langmead, S.L. Salzberg, HISAT: a fast spliced aligner with low memory requirements, Nat. Methods 12 (2015) 357–360.
[28] D. Kim, S.L. Salzberg, Tophat-fusion: an algorithm for discovery of novel fusion transcripts, Genome Biol. 12 (2011) R72.
[29] X.O. Zhang, R. Dong, Y. Zhang, J.L. Zhang, Z. Luo, J. Zhang, L.L. Chen, L. Yang, Diverse alternative back-splicing and alternative splicing landscape of circular RNAs, Genome Res. 26 (2016) 1277–1287.
[30] M.D. Robinson, D.J. McCarthy, G.K. Smyth, edgeR: a Bioconductor package for differential expression analysis of digital gene expression data, Bioinformatics 26 (2010) 139–140.
[31] S. Zhang, M.Y. Xing, G.J. Chen, L. Tong, H.L. Zhang, D.S. Du, Up-regulation of miR-335 and miR-674-3p in the rostral ventrolateral medulla contributes to stress-induced hypertension, J. Neurochem. 161 (2022) 387–404.
[32] L.S. Kristensen, M.S. Andersen, L.V.W. Stagsted, K.K. Ebbesen, T.B. Hansen, J. Kjems, The biogenesis, biology and characterization of circular RNAs, Nat. Rev. Genet. 20 (2019) 675–691.
[33] C.Z. Ren, Z.T. Wu, W. Wang, X. Tan, Y.H. Yang, Y.K. Wang, M.L. Li, W.Z. Wang, SIRT1 exerts anti-hypertensive effect via FOXO1 activation in the rostral ventrolateral medulla, Free Radic. Biol. Med. 188 (2022) 1–13.
[34] X. Tan, P.L. Jiao, J.C. Sun, W. Wang, P. Ye, Y.K. Wang, Y.Q. Leng, W.Z. Wang, β-Arrestin1 reduces oxidative stress via Nrf2 activation in the rostral ventrolateral medulla in hypertension, Front. Neurosci. 15 (2021), 657825.
[35] Y. Hirooka, Oxidative stress in the cardiovascular center has a pivotal role in the sympathetic activation in hypertension, Hypertens. Res. 34 (2011) 407–412.
[36] Y.X. Zhong, Y.J. Du, X. Yang, Y.Z. Mo, C.M. Fan, F. Xiong, D.X. Ren, X. Ye, C.W. Li, Y.M. Wang, et al., Circular RNAs function as ceRNAs to regulate and control human cancer progression, Mol. Cancer 17 (2018) 79.
[37] S.Y. Ren, P.R. Lin, J.R. Wang, H.Y. Yu, T.T. Lv, L. Sun, G.H. Du, Circular RNAs: promising molecular biomarkers of human aging-related diseases via functioning as an miRNA sponge, Mol Ther Methods Clin Dev 18 (2020) 215–229.
[38] Y.K. Gao, S. Katyal, Y.S. Lee, J.F. Zhao, J.E. Rehg, H.R. Russell, P.J. McKinnon, DNA ligase III is critical for mtDNA integrity but not Xrcc1-mediated nuclear DNA repair, Nature 471 (2011) 240–244.
[39] E. Bonora, S. Chakrabarty, G. Kellaris, M. Tsutsumi, F. Bianco, C. Bergamini, F. Ullah, F. Isidori, I. Liparulo, C. Diquigiovanni, et al., Biallelic variants in LIG3 cause a novel mitochondrial neurogastrointestinal encephalomyopathy, Brain 144 (2021) 1451–1466.
[40] M. Akbari, G. Keijzers, S. Maynard, M. Scheibye-Knudsen, C. Desler, I.D. Hickson, V.A. Bohr, Overexpression of DNA ligase III in mitochondria protects cells against oxidative stress and improves mitochondrial DNA base excision repair, DNA Repair 16 (2014) 44–53.
[41] H.L. Sanger, G. Klotz, D. Riesner, H.J. Gross, A.K. Kleinschmidt, Viroids are single-stranded covalently closed circular RNA molecules existing as highly base-paired rod-like structures, Proc. Natl. Acad. Sci. USA 73 (1976) 3852–3856.
[42] X.L. Chen, M. Zhou, L. Yant, C. Huang, Circular RNA in Disease: Basic Properties and Biomedical Relevance, vol. 13, Wiley Interdiscip Rev RNA, 2022, e1723.
[43] P.G. Guyenet, The sympathetic control of blood pressure, Nat. Rev. Neurosci. 7 (2006) 335–346.
[44] Y. Hirooka, Oxidative stress in the cardiovascular center has a pivotal role in the sympathetic activation in hypertension, Hypertens. Res. 34 (2011) 407–412.
[45] G. Li, L.H. Zhang, miR-335-5p aggravates type 2 diabetes by inhibiting SLC2A4 expression, Biochem. Biophys. Res. Commun. 558 (2021) 71–78.
[46] X.K. Lu, Y. Li, H.M. Chen, Y.C. Pan, R. Lin, S.Y. Chen, miR-335-5P contributes to human osteoarthritis by targeting HBP1, Exp. Ther. Med. 21 (2021) 109.
[47] L.L. Ye, F. Wang, H. Wu, H. Yang, Y. Yang, Y.J. Ma, A.L. Xue, J. Zhu, M.L. Chen, J. Y. Wang, et al., Functions and targets of miR-335 in cancer, OncoTargets Ther. 14 (2021) 3335–3349.
[48] Y.X. Liu, J.Y. Yang, X. Yang, P. Lai, Y. Mou, J.L. Deng, X.Y. Li, H. Wang, X.L. Liu, L. X. Zhou, et al., H2O2 down-regulates SIRT7's protective role of endothelial premature dysfunction via microRNA-335-5p, Biosci. Rep. 42 (2022), BSR20211775.
[49] Y.X. Liu, P. Lai, J.L. Deng, Q.K. Hao, X.Y. Li, M. Yang, H. Wang, B.R. Dong, MicroRNA335-5p targeted inhibition of sKlotho and promoted oxidative stress-mediated aging of endothelial cells, Biomarkers Med. 13 (2019) 457–466.
[50] E.P. Murchison, G.J. Hannon, miRNAs on the move: miRNA biogenesis and the RNAi machinery, Curr. Opin. Cell Biol. 16 (2004) 223–229.
[51] P.J. Connelly, G. Currie, C. Delles, Sex differences in the prevalence, outcomes and management of hypertension, Curr. Hypertens. Rep. 24 (2022) 185–192.
[52] L. Te Riet, J.H. van Esch, A.J. Roks, A.H. van den Meiracker, A.H. Danser, Hypertension: renin-angiotensin-aldosterone system alterations, Circ. Res. 116 (2015) 960–975.
[53] H. Kumagai, N. Oshima, T. Matsuura, K. Iigaya, M. Imai, H. Onimaru, K. Sakata, M. Osaka, T. Onami, C. Takimoto, et al., Importance of rostral ventrolateral medulla neurons in determining efferent sympathetic nerve activity and blood pressure, Hypertens. Res. 35 (2012) 132–141.
[54] B. Shell, K. Faulk, J.T. Cunningham, Neural control of blood pressure in chronic intermittent hypoxia, Curr. Hypertens. Rep. 18 (2016) 19.